Available online at www.sciencedirect.com

ScienceDirect

journal homepage: www.elsevier.com/locate/bbe

Original Research Article

A novel method to design an electro-kinetic platform based on complementary metal-oxide semiconductor technology using SKILL scripting of cadence

Reda Abdelbaset [a,b,*], *Yehya H. Ghallab* [a,b,c], *Yehea Ismail* [b]

[a] *Biomedical Engineering Department, Helwan University, Cairo, Egypt*
[b] *Center of Nano Electronics and Devices (CND), Zewail City of Science and Technology and The American University in Cairo (AUC), Cairo, Egypt*
[c] *Electronics and Communication Engineering Department (ECE), Kuwait College of Science and Technology, Kuwait*

ARTICLE INFO

Article history:
Received 12 February 2018
Received in revised form
4 August 2018
Accepted 25 November 2018
Available online 3 December 2018

Keywords:
Dielectrophoresis
Electro-kinetic
Traveling
Levitation
SKILL scripting of cadence

ABSTRACT

The dielectrophoresis (DEP) is the motion of polarizable particles which is a result of the interaction between a non-uniform electric field and the induced dipole moment of these particles. The electro-kinetic DEP is a widely used technique for biological cells' manipulation, characterization and separation. The electro-kinetic DEP consists of three major configurations, they are; traveling wave dielectrophoresis (twDEP), electro-rotation dielectrophoresis (rotDEP), and levitation (levDEP). In this paper, a design of electrokinetic platform that includes the three electrokinetic configurations is presented and discussed. The design of the electrokinetic platform is implemented and simulated using 130 nm complementary metal-oxide-semiconductor (CMOS) technology. Also, this paper presents a developed technique to design the electrokinetic platform's electrodes. This developed technique is the usage of SKILL scripting of cadence (SSC) language. CMOS is a technology which is used to fabricate integrated circuits (IC). SKILL is a scripting language which supports the automation of a specific layout design by commands. The layout of electrokinetic DEP platform is developed using SSC. The performance of the developed electrokinetic platform using SSC versus the platforms based on the other traditional techniques is presented and evaluated using COMSOL Multiphysics®.

* *Corresponding author at*: Center of Nano electronics and Devices (CND), Zewail City of Science and Technology and The American University in Cairo (AUC), Cairo, Egypt.
https://doi.org/10.1016/j.bbe.2018.11.011
0208-5216/

1. Introduction

The dielectrophoresis phenomenon became a well-known method in separation and manipulation of biological particles, in which a non-uniform electric field exerts a net force on the induced dipole of particles [1–3]. The direction and magnitude of DEP force depend on the electric field (frequency, amplitude, and waveform), the size of a particle, and the dielectric properties of the particles comparative to the surrounding medium [4]. Electrokinetic broadly is the motion of polarizable particles immersed in a fluid as a result of the applying of a nonuniform electric field. Electrokinetic technique consists of three major configurations, which are traveling wave dielectrophoresis (twDEP) [5], electrorotation dielectrophoresis (rotDEP) [5], and levitation dielectrophoresis (levDEP) [3].

CMOS is a technology which is used to fabricate integrated circuits (IC) [6]. It is widely used in many fields and applications such as: microprocessors, microcontrollers, static RAM, and other digital logic circuits. Furthermore, it is also used in a wide variability of analog circuits as follows: physical sensors, image sensors, and highly integrated transceivers for many types of communication [6]. Two important advantages of CMOS devices are high noise immunity and low static power consumption [7]. Many scientific groups and researchers have started to use the CMOS technology in lab-on-a-chip applications [8,9]. SKILL is a scripting language which supports the automation of a specific layout design by commands [10].

In this paper, a developed electro-kinetic platform is implemented using complementary metal-oxide semiconductor (CMOS) technology with the aid of SKILL scripting of cadence. The dielectric properties within a specific range of frequencies are used to distinguish between different types of biological cells, such as normal, and lesions cells [3]. On the other hand, microbeads are glass microspheres which are used to emulate the real microbiological particles in terms of dielectric properties. Microbeads are used to test the capability and the performance of DEP based platforms [11].

Contrary the electrophoresis force, DEP requires a nonuniform electric filed to be applied to observe the effects of DEP phenomena. The governing vector relationship defining the DEP force is FDEP = $(\rho \cdot \nabla)E$, where ρ is the effective polarization induced in the particle, ∇ is the gradient operator and E is non-uniform electric field intensity [3]. Traveling wave DEP (twDEP) is obtained as a result of a non-uniform electric field generated from a sequence of signals shifted by 90° phase difference that are applied to a microelectrode array, an induced DEP force observed on particles resulting from twDEP [12]. Similarly, levitation DEP force can be obtained [3].

Concentric electrode rings are the preferred design for twDEP force [5,13], as shown in Fig. 1A. While, quadrupole electrodes are the preferred design for levDEP force [3,14], as shown in Fig. 1B.

In this work, a novel method for designing complex shapes of microelectrodes for several applications (especially biomedical) is presented, described and discussed. This novel method allows designers to implement their designs efficiently, accurately and very quickly.

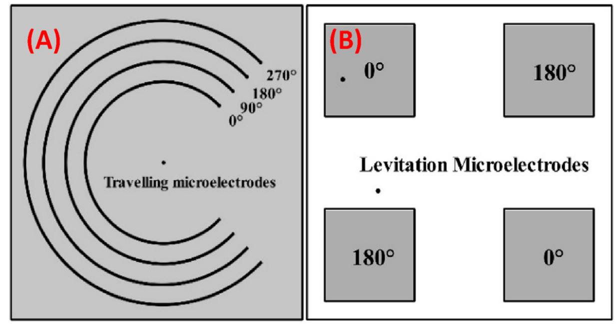

Fig. 1 – A simple layout of: (A) traveling microelectrodes; (B) levitation microelectrodes.

2. SKILL scripting for designing electro-kinetic platform

The proposed electro-kinetic microelectrodes are designed on cadence (UMC 130 nm CMOS Technology) using SKILL scripting of cadence. This technique is preferred due to various advantages, such as: (1) the ability to draw the proposed microelectrodes array with high accuracy, (2) high accuracy to adjust the position of each part, (3) the ability to adjust the dimensions of electrodes and spaces in between with high accuracy unlike direct drawing, and (4) very efficient in drawing array of elements. SSC's main contribution is the drawing of a specific shapes of microelectrode configuration, whether ring or square with high efficiency and avoiding errors of Design Rule Check (DRC). In [5], the concentric rings were drawn in a layout using polygon conversion process [5]. Where, all curves are converted to line segments that approximate their original shape. The number of line segments used in this conversion is defined by the designer. The levitation electrodes were drawn in a layout based on an octagon shape [15], where, the authors designed the octagon shape using a grid arrangement of metal2 rectangles. In this paper, the concentric rings and levitation electrodes are drawn by an array of specific elements for each configuration which will be explained in the next sections.

2.1. TwDEP electrodes design

The concentric rings have been drawn by arcs; each arc includes an array of specific elements. Fig. 2A shows the shape of a single element. The proposed element consists of a square and two polygons at corners, this shape is preferred to solve most of DRC errors that can be found, such as grid off error and 135° corner error, etc. The position of each arc element in each ring is determined using the following equation:

$$x = R \cos \frac{\theta\pi}{180} \tag{1}$$

$$y = R \sin \frac{\theta\pi}{180} \tag{2}$$

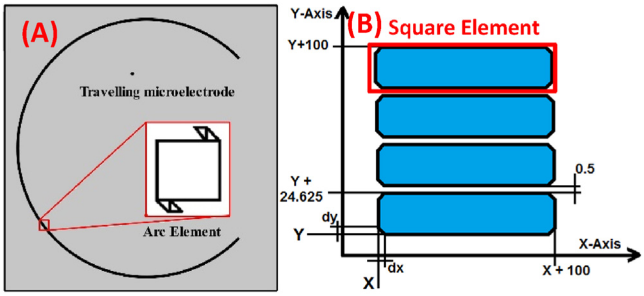

Fig. 2 – (A) Arc element (a unit element within an array to draw an arc (traveling microelectrodes)); (B) square element within single pole of levitation quadrupole.

where x, y are the coordinates of the element position, R is the radius of a ring and θ is the angle of each single element.

Eqs. (1) and (2) have several challenges, such as (1) limitation to change the number of elements in each ring, as the most ring needs a collection of elements more than the least ring to save the same number of elements per length. (2) The size of the element must be variable to keep the same thickness of the ring. (3) The sharpness of element's corners. Overcome the challenges above Eqs. (1) and (2) are developed and implemented based on SSC as shown in Fig. 3.

Fig. 3 shows the flowchart of skill program that is used to implement the concentric rings on cadence. Where, **m** is the number of rings. **S** is a variable number to adjust the number of elements in each ring related to the radius of arc. **A** is a constant to decrease the effect of **J** (Counter). **G** is a constant number of elements in the first ring. **E** is the start angle of arc. **F** is the final angle of arc. **Th** is a constant size of element at x and y-axis. **K** is a variable size of element to adjust the thickness of an arc related to the angle of an element. **R** is the radius of an arc. **H** is the space in between two successive arcs and finally **X** and **Y** are the coordinates of the element position.

Before drawing, the cell view and the layer of metal must be defined in which the electrodes will be built. The cell is defined by the sentence: **CV = degeteditcellview ()**, and the layer of metal is defined by the sentence: **drawlayer = ("ME6" "drawing")**. The rectangle in SKILL is drawn by the sentence: **dbcreaterect(CV drawlayer list(x1:y1 × 2:y2))**, where (x1,y1) the start point of rectangle, while (x2,y2) the end point of rectangle. The polygon in SKILL is drawn by the sentence: **dbcreatepolygon (CV drawlayer list (x1:y1 × 2:y2 . . .. . . xn:yn))**. The script in Fig. 3 is preferred to overcome the challenges of Eqs. (1) and (2) as follows:

1) The density of each ring is improved by increasing the number of elements in each ring as the radius of ring increasing.
2) The thickness of each ring is fixed by changing the size of an element according to its angle.
3) A polygon is added at two opposite corners according to their positions to smooth the circles.

For cadence (UMC 130 nm CMOS Technology), the rings are drawn in metal 7 and connected to bonding pads, for the external interface via connections in metal 6 and 5.

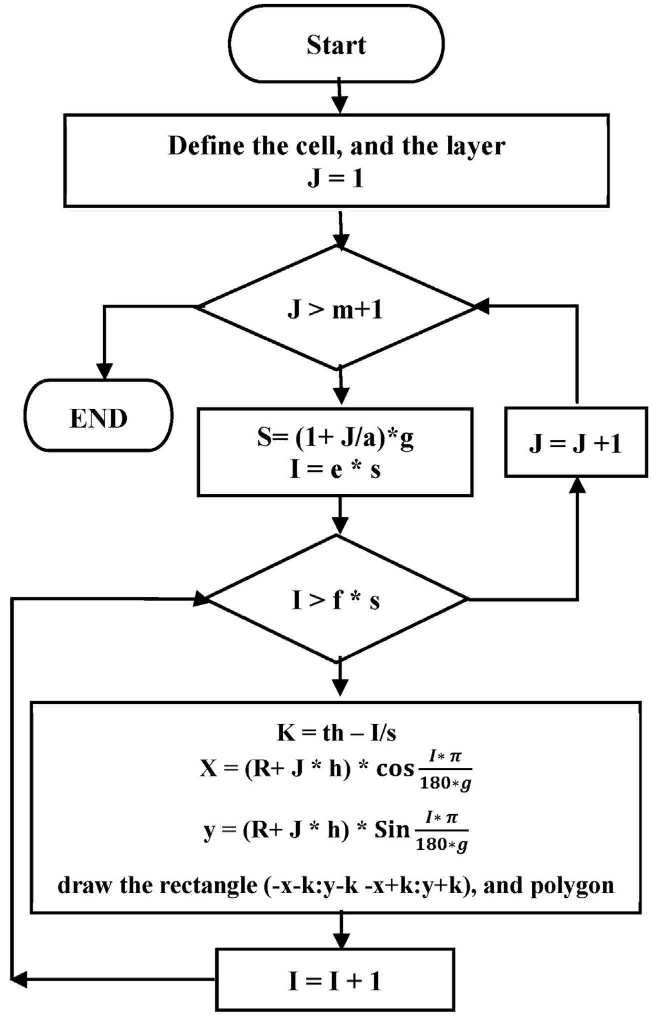

Fig. 3 – Flow chart of skill scripting for designing an arc (element of traveling microelectrodes).

2.2. *LevDEP electrodes design*

The quadrupole levitation configuration consists of four poles, where each pole was drawn by four rectangles, each one has 45° in all corners and size 24.625 × 100 μm to avoid DRC errors. The space in between two successive rectangles is 0.5 μm, therefore the whole dimension of one pole is 100 × 100 μm as shown in Fig. 2B.

Fig. 3 shows the flowchart of skill scripting that is used to implement a single pole of quadrupole levitation electrodes. There are two main challenges according to DRC errors, they are: (1) the corners must be 135°, and (2) the area (x * y) of any block must not exceed ($0 < x <= 25$ μm * $y > 0$) or ($x > 0$ * $0 < y <= 25$ μm). Consequently, the script in Fig. 4 is preferred to design a square which consists of an array of small elements as shown in Fig. 2B. From Fig. 2B, the square element is a rectangle with 45° corners which is drawn by two points with difference Δ in x, and y directions at each corner. In order to

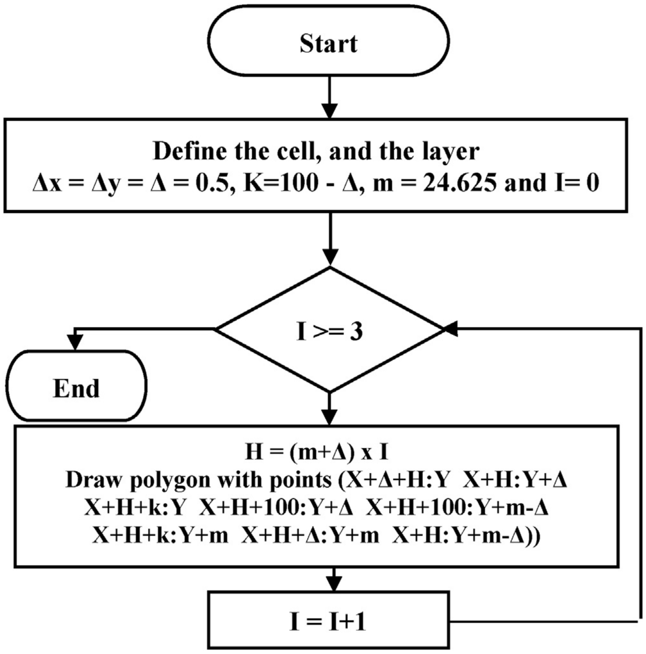

Fig. 4 – Flow chart of skill scripting for designing a single pole of levitation electrode configuration.

preserve the pole with the same dimension; the distance between two elements is taken into account (i.e., it is subtracted from the width of element to be $m = 25 - \Delta/2$). Furthermore, H represents the height of each element, while, K represents the length of element. To draw the whole quadrupole levitation configuration in the layout of cadence, the pole is built by 4 elements ($I = 0$ to $I = 3$), then it is mirrored with specific space to build the four poles with size 100×100 μm and internal space 100 μm.

3. Model of the electrokinetic platform

COMSOL Multiphysics 5.0 is chosen for simulating the electrokinetic platform and microbeads to compare between the proposed platform using SSC and other currently used techniques (such as: polygon conversion, and octagon shape). The model is divided into two major stages. First stage, the preprocessing stage, it includes space dimension, applied physics and study. Second stage, the processing stage which includes the geometry, materials and applied physics conditions as shown in Fig. 5.

The preprocessing stage includes: (1) selection of space dimensions, where 2D is preferred for levitation microelectrodes.

However, the geometry of polygonal concentric rings is difficult to be built on 2D, therefore, 3D is used for traveling microelectrodes. (2) Selection of physics, the electric current module is used to simulate the applied electrical potential and the generated electric field. Frequency domain study is used to calculate the generated electric field at a specific frequency. The creeping flow is used to simulate the medium of particles.

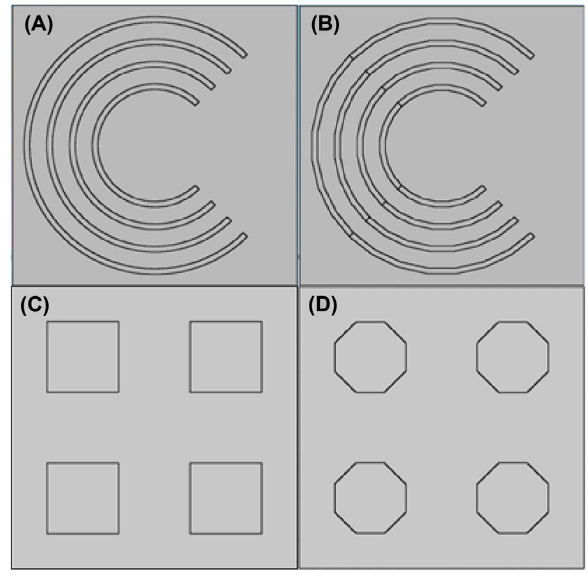

Fig. 5 – The geometry of: (A) concentric rings based on cadence SKILL scripting; (B) polygonal concentric rings; (C) quadrupole based on SSC; (D) octagon quadrupole.

Particle tracing for fluid flow is used to simulate microbeads and calculate the induced DEP force on particles. Time-dependent study is used to identify the change in the induced DEP force on microbeads over time.

The processing stage includes:

(1) geometry: for traveling concentric ring configuration, the model divided into two shapes of rings to compare between them, the first shape is curved rings which is proposed, and the second shape is polygonal rings as shown in Fig. 5A and B, respectively, where each one consists of concentric rings. However, Fig. 5C and D shows the preferred quadrupole design and octagon quadrupole design, respectively.
(2) Defining of materials properties: where, copper is chosen for microelectrodes, FR-4 material is chosen for PCB substrate, deionized water is chosen for medium of particles, and microbeads is chosen for particles [13,14].
(3) Applied physics: creeping flow to simulate the fluid properties of medium, particle tracing to simulate the motion of particles, and electric currents to simulate the generated electric field that is produce by microelectrodes. For traveling, 10 V, 100 kHz square wave signal with phase sequence [0,90,180,270] is used. For levitation, 10 V, 100 kHz square wave 0° phase shift is applied on two opposite squares and 180° phase shift is applied on the other opposite squares.
(4) Mesh: normal physics-controlled mesh is applied.

4. Results

In this section, simulation results of each configuration are presented and discussed. Furthermore, snapshots of the cadence layout of the proposed microelectrodes based on SSC technique are presented.

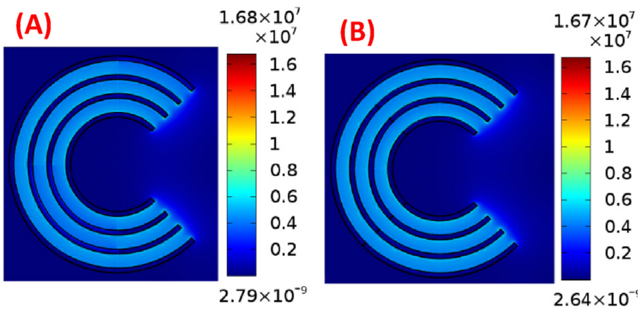

Fig. 6 – The distribution of the electric field strength that is generated by: (A) concentric rings based on cadence SKILL scripting; (B) polygonal concentric rings.

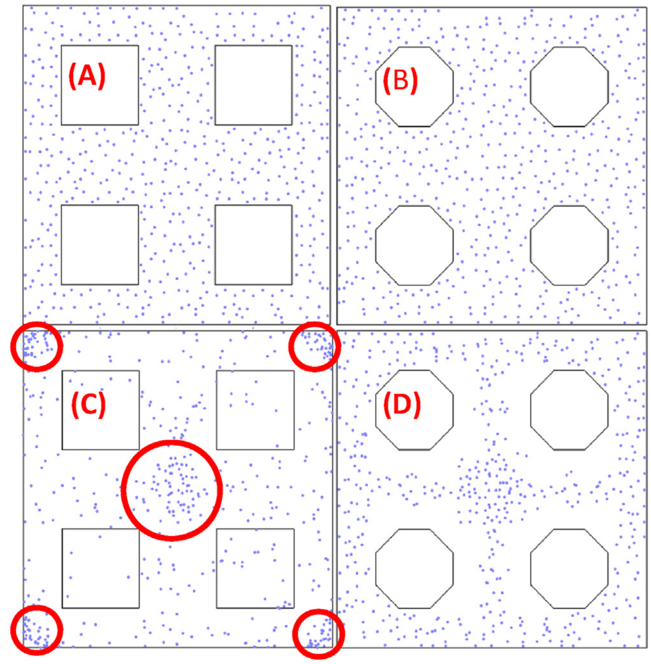

Fig. 8 – The spread of microbeads: (A) over quadrupole based on SSC before applying electric field; (B) over octagon quadrupole before applying electric field; (C) over quadrupole based on SSC after applying electric field; (D) over octagon quadrupole after applying electric field.

A comparison between twDEP microelectrodes using the proposed SKILL scripting method and the traditional polygonal microelectrodes is presented in Fig. 6.

As shown in Fig. 6A and B, the range of the legend bar of electric field strength in case of proposed concentric rings based on SSC is slightly greater than the other one in case of polygonal concentric rings. Consequently, the proposed curved concentric rings design based on SSC is better than the polygonal concentric rings design. A comparison between levDEP microelectrodes using the proposed SKILL scripting method and the traditional octagon microelectrodes using 2D, and 1D plot is presented in Fig. 7. As shown in Fig. 7C, the 1D plot along the line between two opposite electrodes as described in Fig. 7A and B shows marked superiority of the strength of the electric field that is generated by levDEP microelectrodes based on cadence SKILL scripting over another one octagon microelectrodes.

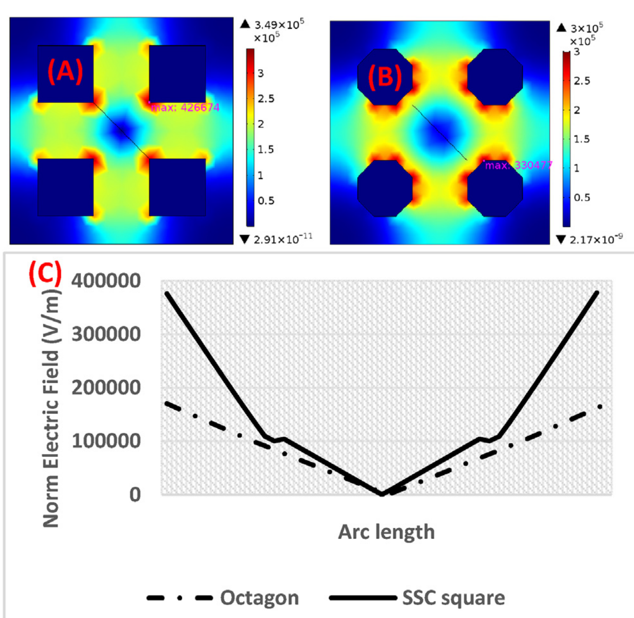

Fig. 7 – The distribution of the electric field strength that is generated by: (A) levDEP microelectrodes based on cadence SKILL scripting; (B) octagon electrodes. While (C) the strength of electric field versus the arc length (the line between the two opposite electrodes as shown in (A) and (B)).

The spread of microbeads over electrodes at different cases is shown in Fig. 8, where Fig. 8A presents the random spread of microbeads over quadrupole levitation electrodes based on SSC at time = 0 s before applying an electric field. Fig. 8C presents the trapping of microbeads over quadrupole levitation electrodes based on SSC at time = 0.01 s after applying an electric field. Fig. 8B presents the random spread of microbeads over octagon quadrupole levitation electrodes at time = 0 s before applying an electric field. Fig. 8D presents the trapping of microbeads over octagon quadrupole levitation electrodes at time = 0.01 s after applying an electric field. Furthermore, in Fig. 8 a comparison between quadrupole levitation electrodes based on proposed method (SKILL scripting of cadence) and octagon quadrupole levitation electrodes in its ability to trap microbeads is presented. Frankly, the main purpose of the quadrupole levitation microelectrodes is trapping cells at specific area for measuring physical features using sensors such as DeFET sensor [12]. Therefore, as shown in Fig. 8C, the red circles prove that the quadrupole levitation electrodes based on SSC are more functional, and efficient to trap microbeads at center area and corners than another one as shown in Fig. 8D.

Fig. 9A and B shows a comparison between the proposed microelectrodes based on SKILL scripting of cadence and traditional octagon microelectrodes in terms of the production of DEP force, and the existed kinetic energy on the particles. The simulation results show a significant advantage of the proposed microelectrodes based on cadence SKILL scripting

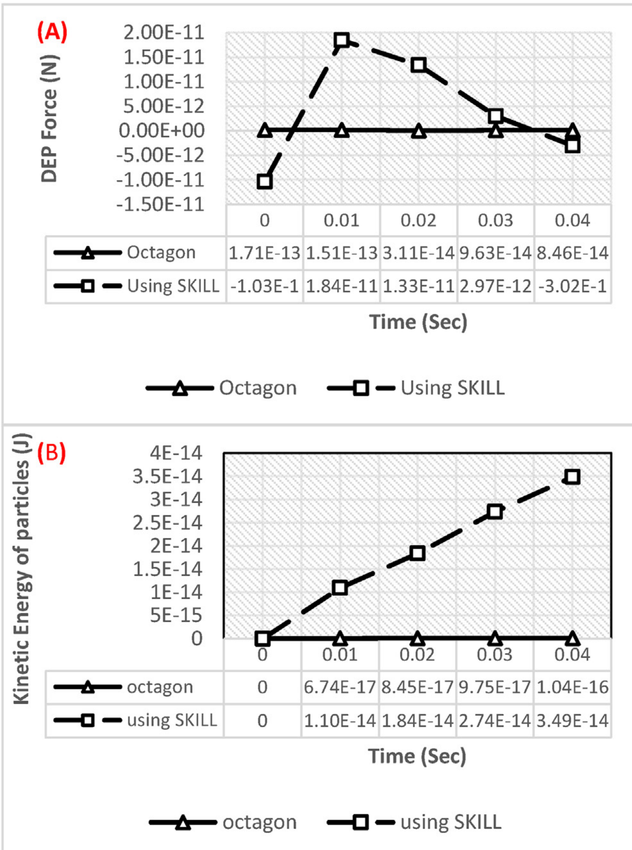

Fig. 9 – A comparison between the proposed microelectrodes based on cadence SKILL scripting and traditional octagon microelectrodes in: (A) the produced DEP force; (B) the existed kinetic energy of particles.

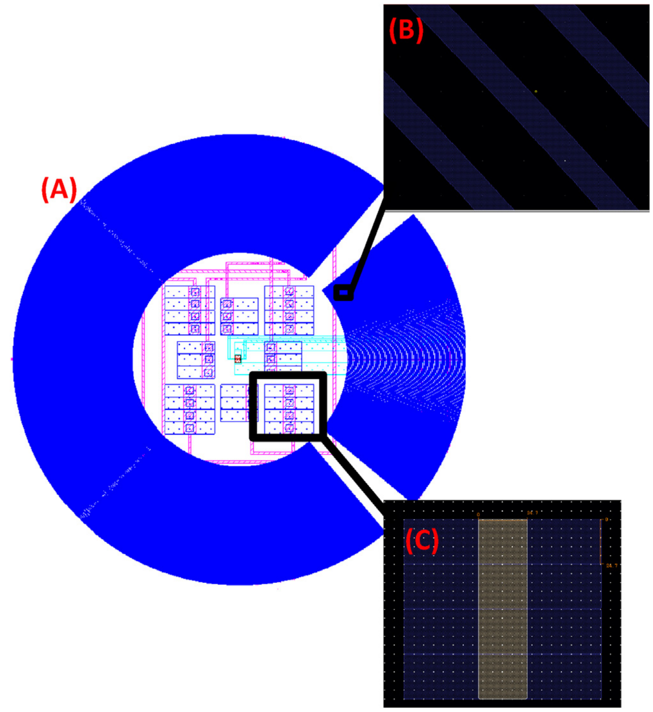

Fig. 10 – snap shots of cadence layout: (A) the proposed microelectrodes using SSC; (B) arcs that are parts of the concentric rings for twDEP electrodes; (C) single pole

over the traditional octagon microelectrodes in both generated DEP force and the existed kinetic energy on particles. Furthermore, Fig. 9A shows a clear superiority of the produced DEP force by the proposed microelectrodes based on cadence SKILL scripting over the produced DEP force by the traditional octagon microelectrodes.

The final layout of the proposed electro-kinetic platform using SSC which combines two configurations (traveling and levitation) is presented in Fig. 10. The proposed electro-kinetic platform is implemented based on two major shapes which are concentric rings for traveling, and quadrupole electrodes for levitation and electro-rotation. As shown in Fig. 10, the concentric rings became more curved after modification using SSC unlike using other methods and single poles became nearly squares after modification using SSC to improve the efficiency of the proposed platform.

Fig. 10B shows sample arcs which are built based on cadence SKILL scripting technique by combining numerous elements with specific dimension and positions as explained previously. However, Fig. 10B shows that the concentric rings based on SSC technique become more curved and smoothed which leads to better performance of the electro-kinetic platform as confirmed by the simulation results.

In Fig. 10C, a single pole for quadrupole levitation configuration is built based on SKILL scripting on cadence by arranging elements with specific dimensions and least possible distances between them. Then, they connected to other elements in other metal layer to act as one pole. The proposed quadrupole configuration based on cadence SKILL scripting became nearly square; therefore, the functionality of the electro-kinetic platform is improved as confirmed by the simulation results.

Finally, Fig. 10 proves that the drawing of complex microelectrodes for biological applications using SSC technique achieves many advantages over the traditional techniques [5,12]. These advantages are as follows: design accuracy in terms of shape (exact rings, exact square) and the positions of microelectrodes without conflict with DRC. In addition to save time and effort because it is able to draw array of many complicated microelectrodes in one step.

5. Conclusion

A novel method to draw the electrodes of an electro-kinetic platform at the layout stage of cadence is presented and discussed. The proposed method uses SSC to improve the performance of the proposed electrokinetic platform. A 2D model of two shapes (polygonal concentric rings and concentric rings based on SKILL scripting of cadence) of traveling configuration is presented and discussed. In addition to, two shapes (quadrupole based on SSC and octagon quadrupole) of levitation configuration using COMSOL is presented and discussed. The layout of cadence after modifying the drawing of electro-kinetic platforms using SSC prove that the rings and squares are implemented efficiently. The simulation results show that the electro-kinetic platform using the proposed method (SKILL scripting of cadence) is better than other designs from previous work. Therefore, the proposed method is a good candidate for designing complex microelectrodes for different applications due to several advantages such as: time saving, high accuracy, and flexibility of code.

Acknowledgement

This research was partially funded by Zewail City of Science and Technology, AUC, the STDF, Intel, Mentor Graphics, ITIDA, SRC, ASRT and MCIT.

REFERENCES

[1] Pohl HA, Pohl HA. Dielectrophoresis: the behavior of neutral matter in nonuniform electric fields. Cambridge: Cambridge University Press; 1978. p. 80.

[2] Eldeeb MA, Ghallab YH, Ismail Y, El Ghitani H. Fully integrated mixed mode interface circuit in 65 nm CMOS for leukemia detection and classification. IEEE International Symposium on Circuits and Systems (ISCAS), May. IEEE; 2018. p. 1–5.

[3] Hartley L, Kaler KV, Luo J, Paul R. Discrete planar electrode dielectrophoresis systems. Electrical and Computer Engineering. Engineering Innovation: Voyage of Discovery. IEEE 1997 Canadian Conference, vol. 1. 1997. pp. 185–92.

[4] Cetin B, Li D. Review dielectrophoresis in microfluidics technology. Electrophoresis 2011;32:2410–27.

[5] Cen EG, Dalton C, Li Y, Adamia S, Pilarski LM, Kaler KV. A combined dielectrophoresis, traveling wave dielectrophoresis and electrorotation microchip for the manipulation and characterization of human malignant cells. J Microbiol Methods 2004;58(3):387–401.

[6] Baker R, Jacob. CMOS: circuit design layout and simulation, vol. 1. John Wiley & Sons; 2008.

[7] Mudanyali O, Mcleod E, Luo W, Greenbaum A, Coskun AF, Hennequin Y, et al. Wide-field optical detection of nanoparticles using on-chip microscopy and self-assembled nanolenses. Nature Photon 2013;7:247–54.

[8] Lu S, Senevirathna B, Dandin M, Smela E, Abshire P. System integration of IC chips for lab-on-CMOS applications. IEEE International Symposium on Circuits and Systems (ISCAS), May. IEEE; 2018. p. 1–5.

[9] Temiz Y, Lovchik RD, Kaigala GV, Delamarche E. Lab-on-a-chip devices: how to close and plug the lab? Microelectron Eng 2015;132:156–75.

[10] Barnes, Timothy J. SKILL: a CAD system extension language. Proceedings of the 27th ACM/IEEE Design Automation Conference. ACM; 1991. p. 266–71.

[11] Spherotech - technical - characteristics of polystyrene particles. Retrieved from: http://www.spherotech.com/particle.html.

[12] Jones TB. Basic theory of dielectrophoresis and electrorotation. Eng Med Biol Magaz IEEE 2003;22(6):33–42.

[13] Abdelbaset R, Ghallab YH, Abdelhamid H, Ismail Y. A 2D model of different electrode shapes for traveling wave dielectrophoresis. 28th International Conference on Microelectronics (ICM), December. IEEE; 2016. p. 257–60.

[14] Abdelbaset R, Ghallab YH, Abdelhamid H, Ismail Y, El-Wakad MT. A 3D model of quadrupole dielectrophoresis levitation. IEEE 59th International Midwest Symposium on Circuits and Systems (MWSCAS), October. IEEE; 2016. p. 1–4.

[15] Ibrahim MF, Ghalab YH, Badawy W. Toward a 3D model of differential electric-field sensitive field effect transistor (DeFET). 1st Microsystems and Nanoelectronics Research Conference, 2008 (MNRC 2008), October. IEEE; 2008. p. 141–4.